Title: High Temperature oxidation evaluation using crystal microbalance

Michael Nicoli[1,2], Francois Grosjean[1], Remy Mingant[1], Jean Kittel[1], Monica Trueba[2], Stefano Trasatti[2], Hubert Perrot[3], Francois Ropital[1],

[1] IFP Energies nouvelles, Rond Point de l'échangeur de Solaize BP3, 69360 Solaize, France
[2] Università degli Studi di Milano,Department of Chemistry,Via Camillo Golgi, 19, 20133 Milano, Italy
[3] Sorbonne Universités, UPMC Université Paris 06, CNRS, Laboratoire Interfaces et Systèmes Électrochimiques, 4, place Jussieu, F-75005, Paris, France.

Corresponding author : Francois Ropital, IFP Energies nouvelles, Rond Point de l'échangeur de Solaize BP3, 69360 Solaize, France email : francois.ropital@ifpen.fr

Abstract. High-temperature oxidising environments are frequently encountered but the limited number of *in situ* techniques that can be implemented has hindered the monitoring possibilities and a better comprehension of the oxidation phenomenon. In this paper the high temperature oxidation behaviours of three alloys (AISI 316L, AISI 310 and HAYNES® HR-120®) were studied by using crystal microbalances and surface characterizations. For the microbalance experiments two types of crystal were tested: quartz or gallium orthophosphate crystals. First the behaviour of thin sputtered deposited alloys on quartz slides was studied at 400 and 700°C under air oxidising conditions and compared to bulk samples. Kinetics measurements were performed on the three alloy films deposited on the resonators at 400 or 700°C under air. After the calibration of quartz and gallium orthophosphate crystals, it was possible to measure very small mass variations associated with thin oxide formation between 5 and 180 nm of thickness. The crystal microbalance technique gives very promising perspectives in understanding the high-temperature corrosion and scaling mechanisms and also for *in situ* monitoring.

Keywords: high temperature corrosion, deposits, crystal microbalance; alloys, corrosion monitoring

1 INTRODUCTION

High-temperature corrosion is an important issue, especially in a crucial field such as energy production. Oxidising environments are frequently encountered as for example in fuel cells, heat exchangers or furnaces. However, the limited number of *in situ* techniques that can be implemented at high temperature has hindered the monitoring possibilities and a better comprehension of the oxidation phenomenon.

In this paper, the feasibility of crystal microbalance as monitoring technique for high temperature oxidation evaluation is considered. The quartz crystal microbalance (QCM) is an extremely sensitive gravimetric device capable of detecting very small mass changes (in the order of ng.cm^{-2}). The operating principle of a QCM is based on the reverse piezoelectric

effect where a voltage is applied across the piezoelectric material resulting in a mechanical strain. The determination of the resonant frequency shift of the crystal after environmental exposure can be related to the mass of the deposit on the crystal.

The QCM has been employed for a broad range of applications such as particle detection, thin-film growth monitoring, surface chemical reaction kinetic studies, materials properties determination and biological sensing. However, in most of those experiments, the resonators were used at or near room temperature (up to 150°C), where the quartz crystals had a low frequency dependence on temperature. Moreover, the SiO_2 crystal could only be used up to the Curie point (573°C) [1], above which it irreversibly loses all piezoelectric properties.

A new material, gallium orthophosphate ($GaPO_4$), is a promising candidate for high-temperature applications [2]. This material is isotypic with quartz [3]. Since the Curie point of the $GaPO_4$ is at 970°C [4], it had been demonstrated the possibility to carry out experiments above 700°C [5]. For these reasons, gallium orthophosphate has recently started being employed to detect carbon deposition onto electrodeposited nickel from methane at 600°C, in order to simulate solid oxide fuel cell anode coking [6], and to measure naphthenic acid corrosion of iron and several alloying elements at 270°C [7].

2 MATERIALS AND METHODS

2.1 Bulk alloy and thin alloy film study

2.1.1 High-temperature exposure of specimens

The materials used in this work were the austenitic stainless steels AISI 310 (UNS S31000), AISI 316L (UNS S31603) and the alloy HAYNES® HR-120® (UNS N08120). The chemical composition of these alloys is given in Table 1.

Table 1. Composition (% by weight) of the different alloys used in this work.

wt.%	Fe	C	Ni	Cr	Mn	Co	Mo	W	Si	Cb	P	S	N	Al	B
316L	Bal.	0,03	10-14	16-18	2	-	2,0-3,0	-	0,75	-	0,045	0,03	0,1	-	-
310	Bal.	0,25	19-22	24-26	2	-	-	-	1,5	-	0,045	0,03	-	-	-
HR-120	33	0,05	37	25	0,7	3	2,5	2,5	0,6	0,7	-	-	0,2	0,1	0,004

All the “bulk” alloys were plate shaped and they were cut by abrasive cutter to obtain square specimens with a surface of about 2x2 cm². Before high-temperature exposures, all the surfaces were polished on SiC paper of decreasing grit size from 180 up to 1200, then ultrasonically cleaned with ethanol, dried in hot air and kept in a desiccator prior to testing.

In order to make a comparison between the behaviour of thin alloy film and bulk alloy, 316L, 310 and HR-120 alloys were deposited on quartz crystals (and also on quartz slides for 316L), using a RF magnetron sputtering reactor (Pfeiffer PLS500). The surface of these specimens was around 3x2 cm² and the thickness of the deposit was about 500 nm. Before

high-temperature exposures, each slide was ultrasonically cleaned in ethanol and dried in hot air.

The exposures under oxidizing atmosphere (air) were performed in a muffle furnace (HERAEUS Thermcon P®). The samples were heated from Room Temperature (RT) up to the desired temperature, with a rate of 5°C/min, in air, and were isothermally oxidized for 24 hours. Then, in the same atmosphere, the samples were left inside the furnace during the natural slow cooling down to RT (around -1.5°C/min).

2.1.3 Surface characterization

The surface of the samples both before and after the tests was examined by an optical microscope (LEICA DM4000 M) and by a stereo microscope (LEICA M165 C).

The microstructure and the composition of the films formed during high-temperature exposures were analysed by scanning electron microscopy (SEM) using a Nova NanoSEM 450 microscope equipped with dispersive X-ray analyser (EDS).

2.2 Microbalance study

2.2.1 Crystals and microbalance

The core of the microbalance was a thin crystal disk with metallic electrodes vapour deposited onto each face of the disk. By applying an alternating electric field through the electrodes, it is possible to induce a mechanical motion inside the crystal around its resonance frequency. In the experiments conducted with the QCM, the measured quantity was the variation of this resonance frequency due to mass changes taking place at the electrode surfaces. The first quantitative correlation between the resonance frequency shifts and the mass deposited on the crystal was established by Sauerbrey [8].

Two types of crystals were used in this work: 9 MHz SiO_2 crystals and 6 MHz $GaPO_4$ crystals. The 9 MHz SiO_2 was manufactured by AWS (Spain) and the 6 MHz $GaPO_4$ crystals by Piezocryst (Austria). All the resonators had the same diameter (14 mm), but different thickness (0.16 mm for the 9 MHz SiO_2 and 0.20 mm for the 6 MHz $GaPO_4$). The quartz crystals had gold keyhole-shaped electrodes deposited onto the two faces of the disks with a titanium adhesion sublayer. Gallium orthophosphate crystals had platinum electrodes with a titanium sublayer (type I) or gold electrodes with a chromium sublayer (type II). For both types of resonators, the piezoelectrically active area had a surface of 0.21 cm^2. Figure 1 gives a schematic view of the SiO_2 and $GaPO_4$ devices.

The frequency changes of the crystals were monitored by a eQCM 10M™ (Gamry Instruments) device coupled with a Gamry Reference 600 potentiostat to carry out the electrochemical calibration tests.

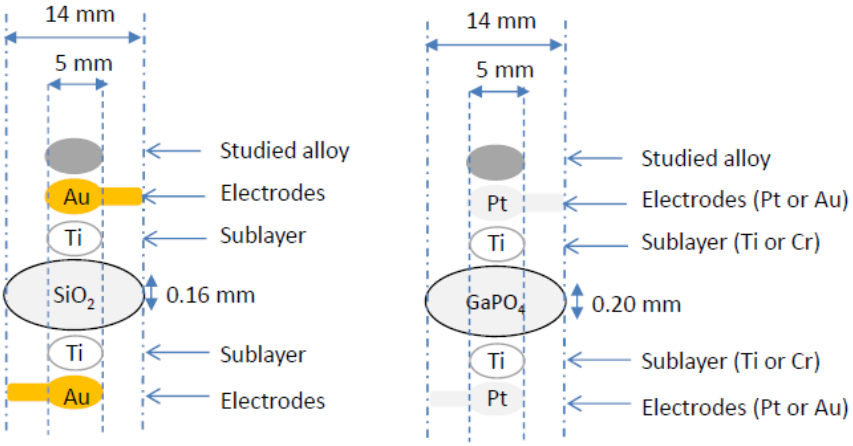

Figure 1. Schematics of the multi-layered crystals

2.2.2 Calibration of crystals

The basic correlation of frequency changes with mass changes is given by the Sauerbrey equation (equation 1):

$$\Delta f = -\frac{2\, n\, f_0^2\, \Delta m}{A\sqrt{\mu_q\, \rho_q}} \qquad (1)$$

where Δf is the frequency shift (Hz), n is the harmonic number of the oscillation ($n = 1$ in our case), f_0 is the fundamental resonance frequency of the crystal (Hz), Δm is the gain or loss of mass (g), A is the piezoelectrically active area (cm^2), μ_q and ρ_q are the shear modulus ($g.cm^{-1}.s^{-2}$) and the density ($g.cm^{-3}$) of the crystal, respectively. The negative sign in the equation indicates that the addition of mass to the resonator results in a decrease in its resonance frequency and vice versa. The equation can also be simplified as:

$$\Delta f = -\frac{K\, \Delta m}{A} \qquad (2)$$

where K is the mass sensitivity coefficient ($Hz.cm^2.g^{-1}$), a constant that contains both the material properties and the fundamental resonance frequency of the crystal. In principle, it is possible to calculate the theoretical value of the sensitivity factor, K^{TH}, for any crystal, by knowing its properties; in practice, it is better to estimate an experimental sensitivity coefficient, K^{EXP}, through simple electrochemical calibration, in order to obtain a more reliable value of this parameter under working conditions.

The 9 MHz SiO_2 and 6 MHz $GaPO_4$ crystals were calibrated by estimating their experimental mass/frequency sensitivity coefficient, K^{EXP}, through galvanostatic copper depositions at different current intensities at room temperature, according to the work of Jakab et al. [9]. A two-electrodes arrangement was employed in a QCM/Static Cell provided by International Crystal Manufacturing. The working electrode was the gold surface of the crystal (0.21 cm^2) and the counter-electrode was a platinum wire. The electroplating solution was made with 0.5 M $CuSO_4$ and 0.5 M H_2SO_4, using reagent grade chemicals. The chemical reaction involved was the copper electrodeposition on the gold electrode, according to the equation 3:

$$CuSO_4(aq) + 2e^- \rightarrow Cu(s) + SO_4^{2-}(aq) \quad (3)$$

The total amount of copper deposited on the gold electrode, Δm_{Cu}, was calculated using the Faraday's law:

$$\Delta m_{Cu} = \frac{I\,\Delta t\,M_{Cu}}{z\,F} \quad (4)$$

where I is the applied current intensity (A), Δt is the electrodeposition duration time (s), M_{Cu} is the copper atomic weight (g mol^{-1}), z is the electrovalence of copper ions (+2) and F is the Faraday's constant (C mol^{-1}). So, the experimental sensitivity factor was obtained by combining equation 2 and equation 4:

$$K^{EXP} = -\frac{\Delta f\ z\ F\ A}{\Delta t\ I\ M_{Cu}} \quad (5)$$

The experimental sensitivity to thermal treatment coefficients calculated for the electrodeposition tests are reported in Table 2. The estimated coefficients were close to the theoretical ones, confirming the validity of the Sauerbrey relationship for these electrodepositions. Moreover, it can be noticed that the experimental coefficient decreased after the heat treatment at 400°C, that meant a reduction of the sensitivity of the device. In Table 3, the values of the coefficients were converted in terms of mass detected for a frequency shift of 1 Hz to easily compare the detection limit of the crystals. The experimental sensitivity given for the quartz resonators were in good agreement with previous results [10].

Table 2. Comparison of the experimental sensitivity factors estimated obtained with SiO_2 and $GaPO_4$ crystals**.**

	K^{TH} (Hz cm^2 g^{-1})	K^{EXP} without HT treatment (Hz cm^2 g^{-1})	K^{EXP} after HT treatment at 400°C (Hz cm^2 g^{-1})
SiO_2	1.83×10^8	$1.62 \pm 0.26 \times10^8$	$1.38 \pm 0.06 \times10^8$
$GaPO_4$	7.68×10^7	$6.87 \pm 0.70 \times10^7$	$6.18 \pm 0.71 \times10^7$

Table 3. Limit of mass detection of SiO_2 and $GaPO_4$ crystals.

	Corresponding mass for 1 Hz shift		
	Δm^{TH} (ng)	Δm^{EXP} without HT treatment (ng)	Δm^{EXP} after HT treatment at 400°C (ng)
SiO_2	1,15	1,29	1,52
$GaPO_4$	2,73	3,06	3,40

2.2.3 High-temperature treatments of different alloys deposited on SiO_2 crystals

The desired alloy (310 or 316L or HAYNES® HR-120®) was deposited onto one gold electrode of the 9 MHz quartz crystals through a RF magnetron sputtering reactor (Pfeiffer PLS500).

The exposures under oxidizing atmosphere (air) were performed in a muffle furnace (HERAEUS Thermcon P®). After the measurement of the resonance frequencies (five acquisitions, 100 s of stabilization, "air mode"), the crystals, without the spring clips, were heated up from RT to the desired temperature, with a rate of 5 °C/min, in air and were isothermally oxidized for a certain time. Then, in the same atmosphere, the resonators were left inside the furnace during the slow cooling down to RT (-1.5 °C/min); the microbalance frequency variations were recorded and the crystals were put again in the furnace for a longer period.

2.2.4 High-temperature tests with $GaPO_4$ crystal

Gallium orthophosphate crystals (type II) were used to carry out high-temperature treatments at 700°C. For these tests, only 316L alloy was used, and was deposited onto one gold electrode, through RF magnetron sputtering technique. The resonance frequency of the crystals was measured three times (100 s of stabilization between each acquisition) in "air mode" before the beginning of the treatments. The crystals, without the spring clips, were put in an alumina boat, heated up from RT to 700°C with a rate of 5°C/min under air in a muffle furnace (HERAEUS thermcon P®) and were isothermally oxidized during a certain period of time (from 30 min for the first test to up to 17 h for the last one). After a slow cooling down to RT (-1.5°C/min), the resonance frequencies were recorded three times (100 s of stabilization) in "air mode" and, then, the cycle was repeated again treating the crystals for a longer period (up to 24 h).

3 RESULTS AND DISCUSSION

3.1 High-temperature oxidation of bulk alloys and thin alloy films

The morphology and the composition of the oxide layers formed on bulk alloys coupons and thin (of about 50 nm thick) deposited films were compared. After the oxidizing treatment, all the specimen surfaces were observed by an optical microscope (OM). The images of the treated quartz slides with 316L film deposit are reported on Figure 2. Changes of colour and morphology on the surfaces were observed.

Moreover, the specimens were weighed before and after the treatments with an analytical balance, but it was not possible to measure a mass variation since the mass gain was below the detection limit of the balance (0.1 mg).

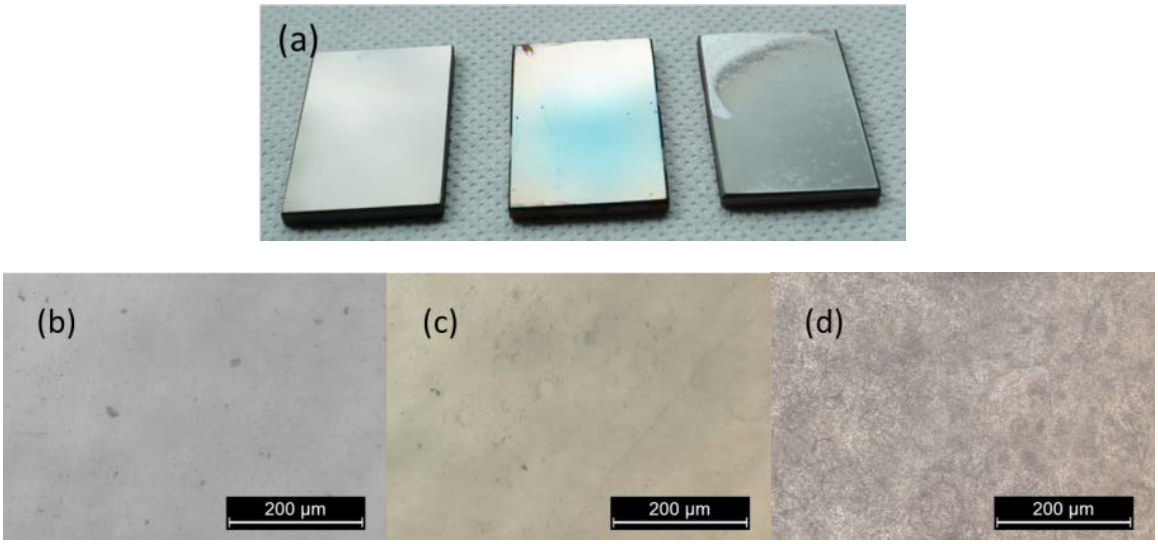

Figure 2. Oxide morphology of 316L SS deposited on quartz slide: (a) photograph of all the slides analysed (from left to right: untreated sample and samples after 24 h of heat treatment at 400°C and 700°C); (b) OM image of the untreated sample; (c) OM image of the sample treated at 400°C; (d) OM image of the sample treated at 700°C.

A detailed assessment of the bulk steel and steel film comparability was obtained through scanning electron microscopy (SEM) and energy-dispersive X-ray spectroscopy (EDS). As shown in Figure 3, the polished 316L SS bulk coupon and the untreated 316L SS thin film deposited on quartz slide have a similar surface morphology. The EDS analysis confirmed that the two samples had the same composition (see Table 4).As the thickness of the steel film was about 0.5 µm, the higher content of oxygen and silicon found into the deposited steel had partially been attributed to the quartz slide onto which the steel was sputtered. Moreover, since the steel film was not polished before the analysis, part of the oxygen content could be due to the atmospheric passivation of the alloy. A similar reactivity between the bulk samples and the sputtered samples could be assumed.

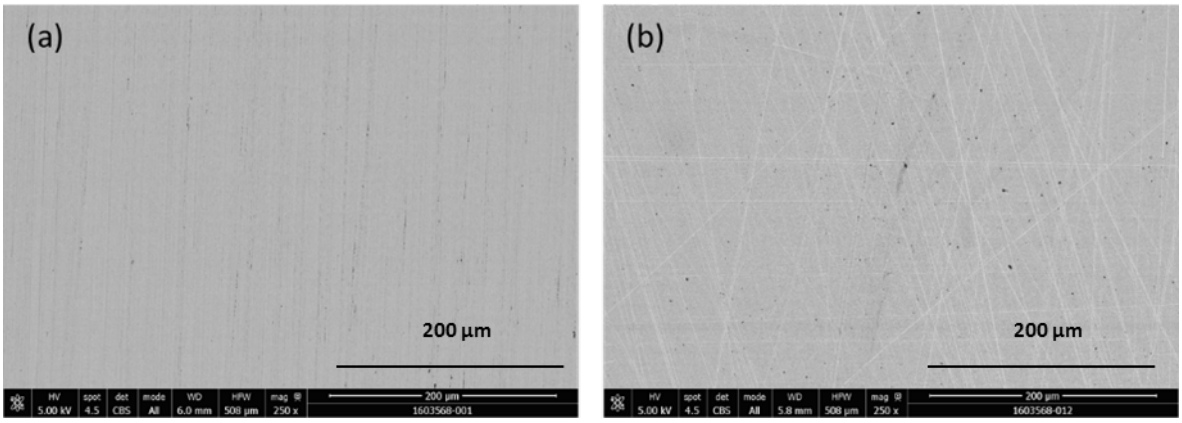

Figure 3 SEM secondary electrons images of 316L SS samples: (a) polished bulk steel coupon; (b) untreated steel film deposited on quartz slide.

Table 4. Composition (% by weight) of the polished 316L SS bulk steel coupon and the untreated 316L SS sputtered on quartz slide.

wt.%	O	Si	Cr	Fe	Ni	Mo
316L	0.6	0.6	17.1	66.6	9.4	1.9
Qslide with 316L	5.4	0.9	15.0	64.2	9.5	1.4

The surface images of 316L samples after 24 h of heat treatment at 400°C are reported in Figure 4. The oxide layers of the bulk steel coupon (Figure 4(a)) and the sputtered steel on quartz slide (Figure 4(b)) were similar in terms of morphology. On the contrary, the steel film deposited on the quartz crystal behaved in a completely different manner, exhibiting a sand-rose-like oxide structure (Figure 4(c) at high magnification and 5(a) and (b) at low magnification). An EDS mapping of the surface of the steel film deposited on the quartz crystal was performed in order to better understand the composition of the oxide layer. In Figure 5(c) the chromium and the oxygen maps are merged. A decrease of chromium and an enrichment in oxygen in correspondence of the sand-rose-like oxide arrangements were observed: these structures should be mixed oxides (spinels), as also indicated by the iron and molybdenum maps.

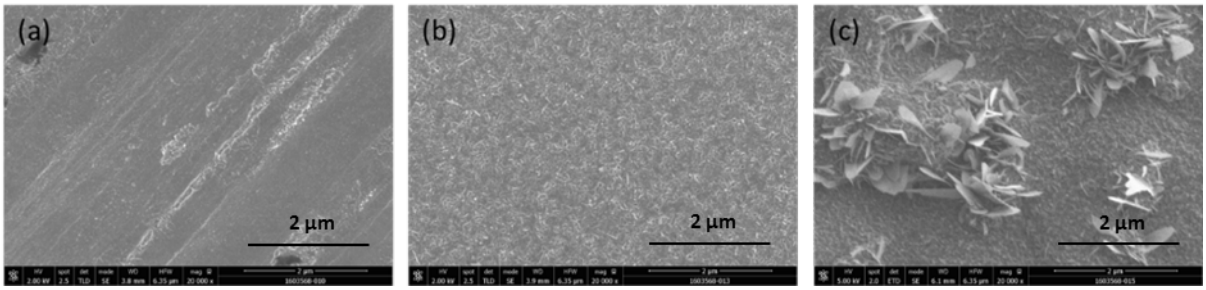

Figure 4. SEM secondary electrons images of the oxides formed after 24 h of heat treatment at 400°C on 316L SS samples: (a) bulk coupon; (b) film deposited on quartz slide; (c) film deposited on quartz crystal.

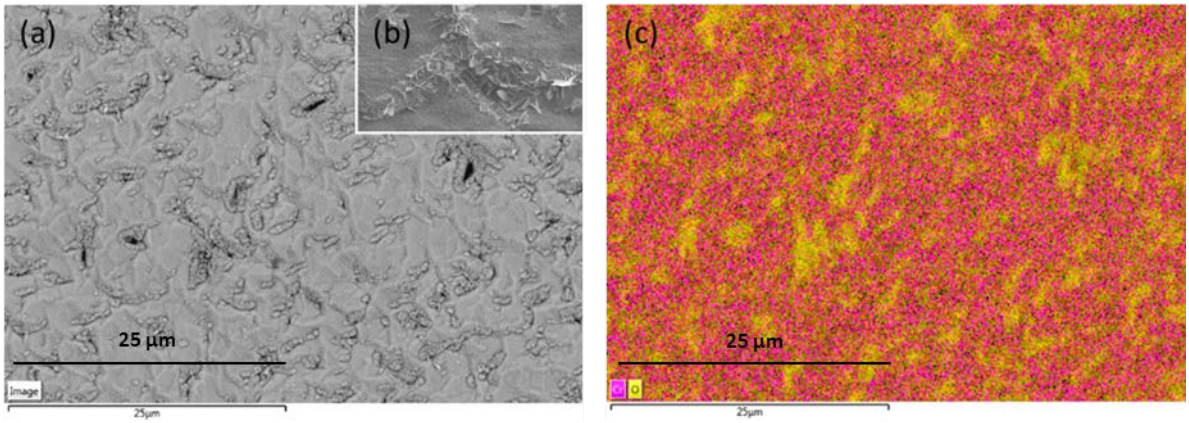

Figure 5. EDS surface mapping of the deposited 316L SS on quartz crystal after 24 h of heat treatment at 400°C: (a) SEM secondary electrons image of the analysed surface; (b) focus on the rose-like oxide structure; (c) Cr (red) and O (yellow) merged map.

The comparison between bulk coupons and thin metal film deposited on quartz crystals was also carried out on 310 SS and HAYNES® HR-120® alloy (Figure 6). As it was observed with the 316 SS, the oxide layers formed on the deposited alloys differ from the ones formed on the bulk specimens, for the same reasons listed above.

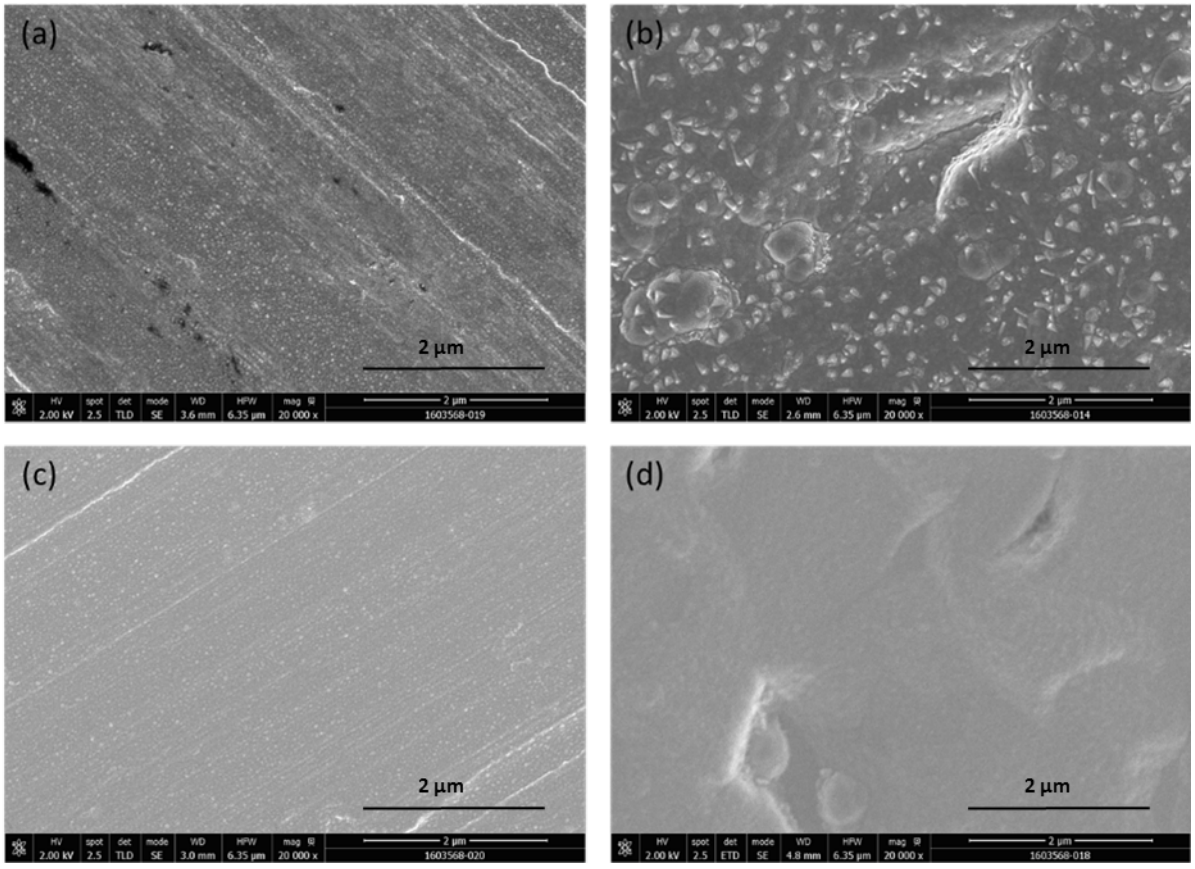

Figure 6. SEM secondary electrons images of the oxides formed after 24 h of heat treatment at 400°C on different samples: (a) 310 SS bulk coupon; (b) 310 SS film deposited on quartz crystal; (c) HAYNES® HR-120® bulk coupon; (d) HAYNES® HR-120® film deposited on quartz crystal.

3.2 High-temperature exposure monitoring by SiO_2 and $GaPO_4$ crystals

3.2.1 Thermal aging of crystals

The evaluation of the impact of high temperature on crystal resonance frequency was attained performing long-term exposures of SiO_2 (9 MHz) and $GaPO_4$ type I (6 MHz) crystals. The treatments were carried out at a fixed temperature (400°C for SiO_2 crystals and 700°C for $GaPO_4$ type I ones), under air, in a muffle furnace (HERAEUS thermcon P®). The resonance frequency of the crystals was measured five times (100 s of stabilization between each acquisition) in "air mode" before the beginning of the treatments (time 0). The resonators, without the spring clips, were put in an alumina boat, heated up from RT to 400°C or 700°C with a rate of 5°C/min and left for a certain period of time (as showing on Figure 7 by the time distance between 2 points). After a slow cooling down to RT (-1.5°C/min), the resonance frequencies were recorded five times (100 s of stabilization) in "air mode" and, then, the cycle was repeated again treating the crystals for a longer period (up to an overall duration of 24h for $GaPO_4$ type I crystals or 120 h for SiO_2 crystals). As shown in Figure 7, after an initial decrease of about 600 Hz, the resonance frequency of the SiO_2 quartz was stable up to 120 hours at 400°C. The $GaPO_4$ crystal exhibited, instead, an increase of resonance frequency of about 1200 Hz after 24 hours at 700°C has shown on Figure 8.

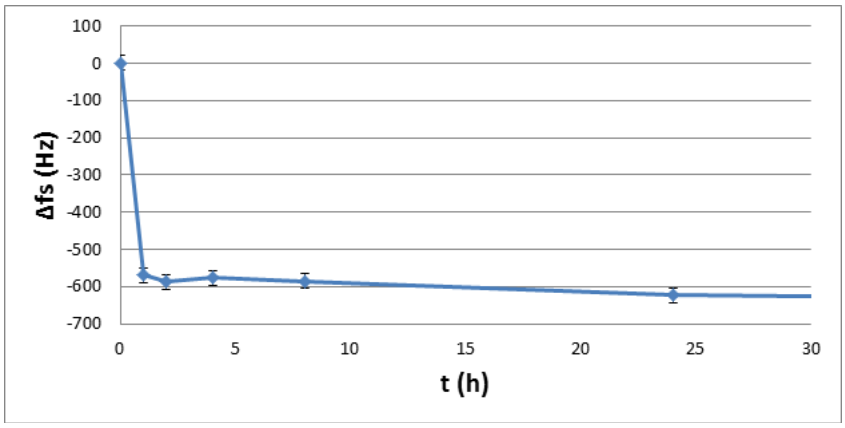

Figure 7. Long-term high-temperature exposures at 400°C of quartz crystal Q5

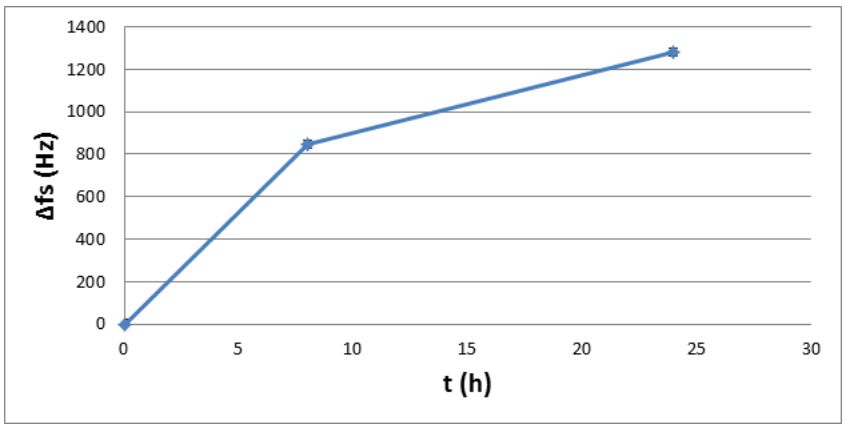

Figure 8. Long-term high-temperature exposures at 700°C of gallium orthophosphate crystal G3

The tests presented above helped to estimate the uncertainty of the measurement. If their number remains limited, the mechanical connections-disconnections of the crystals led to a small uncertainty, around few tens of ng. The main uncertainty could come from the shift due to thermal treatment which could correspond to several hundreds of ng. As a result of these tests, a conservative relative error of 15 % was used on the next plots.

3.2.2 High-temperature oxidation monitoring by SiO_2 crystal

Once the sensitivity coefficient was determined and the preliminary tests were done in order to take into account the blank tests, 9 MHz quartz crystals were used to detect the thin oxide film formation of three different types of alloys at 400°C under oxidizing (air) atmosphere.

Three quartz crystals Q8, Q12 and Q15, with 316L, 310 and HAYNES® HR-120® deposits, respectively, underwent a heat treatment at 400°C in air. Figure 9 shows the mass variation and the error bars of the deposited alloys over time during the heat treatment. For all the alloys, the mass gains increased over the time following a parabolic law, as expected for an oxidation kinetics controlled by the diffusion of cationic and anionic species through the surface layer. It was noticed that the 316L SS formed a higher amount of oxide in respect to the 310 SS and the HAYNES® HR-120® alloy. The mass gain was calculated from the frequency variation of a crystal through the equation 6:

$$\Delta m = -\frac{\Delta f \, A}{K_Q^{EXP}} \tag{6}$$

where $K_Q^{EXP} = 1.38 \cdot 10^8$ Hz.cm^2.g^{-1} and $A = 0.21$ cm^2.

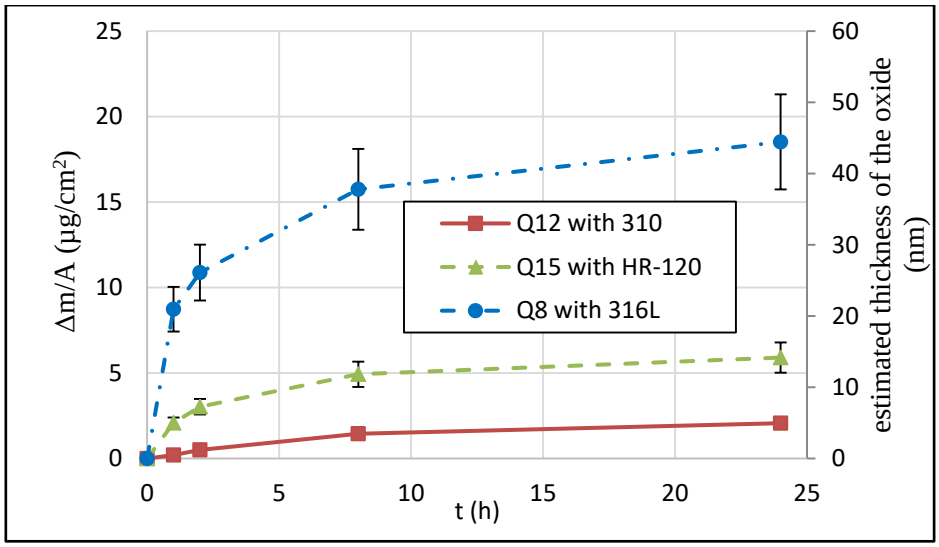

Figure 9. Mass variation of different type of alloys deposited on quartz crystals during oxidizing treatment.

By assuming that the oxide was only composed of Cr_2O_3 which had a 5.21 g/cm^3 density, the estimated oxide thickness was calculated from the mass gains. After 24 hours of oxidation under air at 400°C, the thickness of the oxide layer was around 5 ±1 nm for AISI 310 steel, 14 nm for HAYNES® HR-120® steel and 45 ±5 nm for AISI 316 steel. The results obtained with the microbalance could also explain why it was not possible to measure the mass variation of the oxidized bulk coupons using the analytical balance. In fact, after 24 h of heat treatment at 400°C, the mass gain of a 316L coupon (12.5 cm^2) was estimated around 300 ± 20 µg.

3.2.3 High-temperature oxidation monitoring by $GaPO_4$ crystal

The gallium orthophosphate crystals (type II), G5 with 316L steel deposit was treated at 700°C in air. After correction of the sensitivity and blank tests results, a mass increase of 95 µg.cm^{-2} after 8 h of oxidation was measured. In the literature [11], parabolic constants Kp= 3 10^{-13} g^2.cm^{-4}. s^{-1} are mentioned for the oxidation of 25 %Cr stainless steels at 700°C. This Kp value led to a mass gain of 93 µg.cm^{-2} for a 8 hours oxidation experiment in good concordance of our experimental results (95 µg.cm^{-2}) and the data from the literature. By assuming that the oxide was only composed of Cr_2O_3 which had a 5.21 g/cm^3 density, the corresponding oxide thickness was around 180 ± 20 nm (for comparison at 400°C on quartz crystal, the oxide thickness on sputtered 316L SS was estimated at 45 nm). With this $GaPO_4$ material, it was possible to characterize oxide layer obtained at higher temperature and to estimate the oxide film thickness with a good sensitivity.

CONCLUSION

In this paper the high temperature oxidation behaviours of three alloys (AISI 316L, AISI 310 and HAYNES® HR-120®) were studied by gravimetric measurements (crystal microbalance to follow *ex situ* the mass variation) and surface characterization (optical and electronic microscopy). For the microbalance experiments two types of crystal were tested: quartz and gallium orthophosphate crystals.

First, the behaviour of thin sputtered deposited alloys on quartz slides was studied at 400°C and 700°C under air oxidising conditions, with no noticeable differences compared to bulk samples.

Kinetics measurements had then been performed on the 316L, 310 and HAYNES® HR-120® alloy films deposited on resonating crystals and treated at 400°C and 700°C under air. After the calibration of quartz and gallium orthophosphate crystals, it was possible to measure very small mass variations associated with the oxide formation between 5 and 180 nm of thickness.

The microbalance technique, thanks to its capability of detecting mass shift in the order of few tens of nanograms, gives very promising perspectives in the study and understanding of high-temperature corrosion and also for *in situ* monitoring.

REFRERENCES

[1] J. W. Elam and M. J. Pellin, "$GaPO_4$ sensors for gravimetric monitoring during atomic layer deposition at high temperatures," *Analytical chemistry*,**77** (2005), 11, 3531-3535

[2] H. Fritze, "High-temperature bulk acoustic wave sensors," *Measurement Science and Technology*, **22** (2011**)** 1, 12002

[3] F. Krispel , C. Reiter , J. Neubig , F. Lenzenhuber , P. W. Krempl , W. Wallnöfer and P. M. Worsch, “Properties and applications of singly rotated $GaPO_4$ resonators,” Conference: Frequency Control Symposium and PDA Exhibition Jointly with the 17th European Frequency and Time Forum, 2003

[4] P. W. Krempl, “Quartzhomeotypic gallium orthophosphate: A new high-tech piezoelectric crystal,” *Ferroelectrics*, **202** (1997) 1, 65-69

[5] J. Haines, O. Cambon, N. Prudhomme, G. Fraysse, D. A. Keen, L. C. Chapon, and M. G. Tucker., “High-temperature, structural disorder, phase transitions, and piezoelectric properties of GaPO4,” *Physical Review B*, **73** (2006) 014103

[6] J, Millichamp, T.J. Mason, N.P. Brandon, R.J.C. Brown, R.C. Maher, G..Manos, T.P. Neville, D.J.L. Brett “A study of carbon deposition on solid oxide fuel cell anodes using electrochemical impedance spectroscopy in combination with a high temperature crystal microbalance,” *Journal of Power Sources*, **235** (2013) 14-19

[7] B. N. Patrick, R. Chakravarti, and T. M. Devine, “An Acoustic Microbalance Study of High-Temperature Naphthenic Acid Corrosion of Common Iron-Alloying Elements,” *Corrosion*, **71** (2015) 9, 1135-1146

[8] G. Sauerbrey, “Verwendung von Schwingquarzen zur Wägung dünner Schichten und zur Mikrowägung,” *Z. Physik (Zeitschrift für Physik)*, **155** (1959) 2, 206-222

[9] S. Jakab, S. Picart, B. Tribollet, P. Rousseau, H. Perrot and C. Gabrielli, “Study of the dissolution of thin films of cerium oxide by using a $GaPO_4$ crystal microbalance,” *Analytical chemistry*, **81** (2009) 13, 5139-5145

[10] K. Bizet, C. Gabrielli and H. Perrot,” Immunodetection by quartz crystal microbalance“, *Applied Biochemistry and Biotechnology*, **89** (2000**)** 139-150

[11] A.J. Felten,” High-Temperature Oxidation of Fe-Cr Base Alloys with Particular Reference to Fe-Cr-Y Alloys” *Journal Electrochemical Society*, **108** (1961) 6, 490-495